Sensors & Actuators: B. Chemical 338 (2021) 129835

Contents lists available at ScienceDirect

Sensors and Actuators: B. Chemical

journal homepage: www.elsevier.com/locate/snb

Highly sensitive detection of rabbit IgG by electron spin resonance using CuS nanoparticles as probe

Sizhu Tian [a], Xuwen Li [a], Jia Jiang [a], Li Tang [a], Hanqi Zhang [a], Yong Yu [b], Ziwei Zhang [a,*]

[a] College of Chemistry, Jilin University, Qianjin Street 2699, Changchun, 130012, PR China
[b] College of Instrumentation and Electrical Engineering, Jilin University, West Minzhu Street 938, Changchun, 130061, PR China

ARTICLE INFO

Keywords:
CuS nanoparticles
Electron spin resonance
Immunoassay
Cu^{2+}-DDC complex
Rabbit IgG

ABSTRACT

Water soluble copper sulfide (CuS) nanoparticles were synthesized using L-cysteine as the ligand. Multiple biotins were conjugated to the antibody of rabbit IgG, and the streptavidin was attached to the CuS nanoparticles. The Cu^{2+} ions enclosed in the nanoparticles were used as the electron spin resonance (ESR) probes and detected with ESR spectrometer. The immunoassay reaction was resulted in the formation of the coating antibody attached to the microplate well, the detecting antibody labeled with the biotins, and the streptavidin attached to the CuS nanoparticles. After the immunoassay reaction was performed, large amount of Cu^{2+}/Cu^{+} ions inside the nanoparticles were released with the help of diethyldithiocarbamate (DDC) and the Cu^{2+}-DDC complex formed. The Cu^{2+}-DDC complex was extracted into *n*-butanol, which was used as the analytical sample. Both ESR and UV–vis signals were collected for the analytical sample. The double logarithm standard curve was well simulated with a linear regression equation. The limits of detection of the rabbit IgG were 1.76 pg/mL and 2.36 pg/mL by ESR and UV–vis method, respectively. The detection range using ESR as the detector was from 8.8 pg/mL to 500 ng/mL, covering almost 5 magnitude orders of the rabbit IgG concentrations. The rabbit serum was analyzed and the rabbit IgG concentration was found to be 7.76 mg/mL. The reproducibility of the present method was good enough with the intra-assay error within 3.4 % and the inter-assay error within 11.2 %. The spiked serum samples were analyzed and the experimental results indicated that the recoveries were from 108.2 to 113.7%.

1. Introduction

Electron spin resonance (ESR), also known as electron paramagnetic resonance (EPR) or electron magnetic resonance (EMR), is a spectroscopic technique that can be applied in the detection of substances containing unpaired electrons. For example, the free radicals such as nitroxide radical (·NO) and hydroxyl radical (·OH) as well as the paramagnetic metal ions such as Mn^{2+}, Gd^{3+}, and Cu^{2+} can all give ESR signals [1,2]. So ESR spectroscopy has been applied in many academic fields including chemistry, life science, food science, physics, and material science [3–5].

Immunoassay is the bioanalytical method based on the reaction between the antigen and the antibody and used in the determination of the compounds or macromolecules in the body fluids at low concentrations [6]. Since 1960s, the scientists have developed many practical immunoassay methods including the very beginning radioimmunoassay (RIA) using the radio-isotope as the label, the most widely used enzyme immunoassay (EIA) using the enzyme instead of radio-isotope as the label, fluoroimmunoassay (FIA) with the fluorophore as the label, chemiluminescence immunoassay (CLIA) with the chemiluminescent agent as the label, electro-chemiluminescence immunoassay (ECLIA), capillary electrophoresis immunoassay (CEIA), and flow-injection immunoassay (FIIA) [7–10]. These immunoassay methods have been successfully applied in many fields such as clinical examination, diagnosis of diseases, pharmaceutical analysis, and industrial quality control. The test objects of these immunoassay methods spread from small molecules such as drugs and hormones to biological macromolecules such as biomarker proteins and enzymes.

The development of ESR technique as an immunoassay method has been launched since 1970s [11]. In most methods, the ESR probes were free radicals and the test objects included both small molecules and macromolecules [12–14]. Although the combination of ESR technique and immunoassay has been proposed for many years, the methods and the publications are still limited. In this paper, a new method using CuS nanoparticles as the ESR probe was proposed.

Due to the quantum confinement phenomenon, CuS nanoparticles

* Corresponding author.
E-mail address: zzw@jlu.edu.cn (Z. Zhang).

https://doi.org/10.1016/j.snb.2021.129835
Received 7 December 2020; Received in revised form 17 March 2021; Accepted 18 March 2021
Available online 22 March 2021

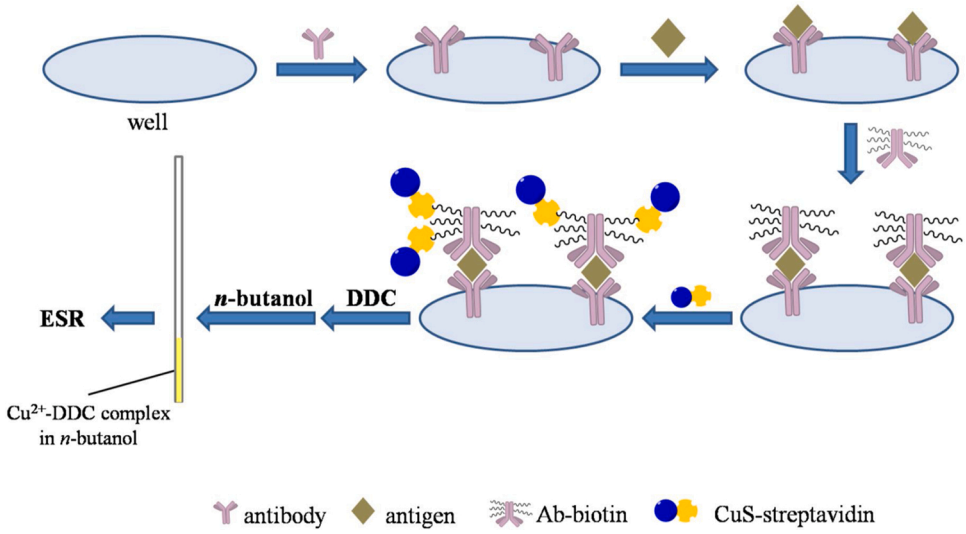

Fig. 1. Schematic diagram of ESR method.

(NPs) exhibit special optical, electrical, and photothermal properties. Because of these good properties as well as the small particle size and low toxicity, CuS NPs have been applied in some areas of biological science such as photothermal therapy, imaging, immunoassay, and small molecule detection [15,16]. Dutta et al. [17] designed a green synthetic method and obtained CuS NPs with intrinsic peroxidase-like activity, which were used as the biosensor for the detection of blood glucose level. Liang et al. [18] conjugated the tumor-targeting ligand on the surface of bovine serum albumin (BSA) capped CuS NPs, and used this nanocomplex in tumor imaging and photothermal therapy. However, up to now, the utilization of CuS NPs in the immunoassay using ESR as the detector has not been reported.

The object of this work is to develop a novel ESR immunoassay method using synthesized CuS NPs as the probe. The biotin-avidin system has been introduced in this method to achieve further signal amplification. Instead of direct measuring the ESR signal of the nanoparticles, the Cu^{2+} ion is released from the nanoparticles with the help of DDC and *n*-butanol and its ESR signal peak is much sharper and higher. Thus the new method is highly sensitive when detecting rabbit IgG with a limit of detection (LOD) as low as 1.76 pg/mL. Compared to our two previous publications also with rabbit IgG as the detection subject but based on iron oxide nanoparticle probe, the detection sensitivity achieved in the present work is improved for 4–5 orders of magnitude. The detection range is wide and a good linear relationship is satisfied. Also the intra- and inter-assay reproducibility, as well as the accuracy obtained from the serum spiking experiments are satisfactory.

2. Experimental section

2.1. Chemicals and materials

Rabbit IgG and goat anti-rabbit IgG polyclonal antibody (Ab) were purchased from Arista Biologicals. Normal rabbit serum was purchased from Shanghai Yeasen Biological Technology Co., Ltd. Biotinamidohexanoyl-6-aminohexanoic acid N-hydroxysuccinimide ester (Biotin-XX-NHS) was purchased from Sigma-Aldrich, Co. Streptavidin was provided by J&K Scientific Ltd. Stripwell high-binding polystyrene microplates were purchased from Corning Inc. Bovine serum albumin (BSA), copper nitrate trihydrate ($Cu(NO_3)_2{\cdot}3H_2O$), dimethyl sulfoxide (DMSO), N-(3-dimethylaminopropyl)-N'-ethylcarbodiimide hydrochloride (EDC), N-hydroxysuccinimide (NHS), 4′-hydroxyazobenzene-2-carboxylic acid (HABA), L-cysteine, 4-(2-hydroxyethyl)-1-piperazineethanesulfonic acid (HEPES), sodium diethyldithiocarbamate (DDC), and Tween-20 were purchased from Aladdin Industrial Co. Sodium sulphide hydrate ($Na_2S{\cdot}9H_2O$) was purchased from Xilong Scientific Co., Ltd. *n*-Butanol, methanol, and sodiom hydroxide (NaOH) were purchased from Beijing Chemical Works. All other reagents were of analytical grade. Ultrapure millipore water (18.2 mΩ) was used.

2.2. Preparation of CuS NPs

The nanoparticles were synthesized using the method describe by Guo et al. [19] with some modifications. Typically, 127.9 mg L-cysteine was dissolved into 386 mL of water in a round bottom flask. Then, 4 mL of $Cu(NO_3)_2$ was added to the reaction mixture with rapid stirring. The pH of the mixed solution was adjusted to 10.1. The mixture was stirred under a nitrogen atmosphere for 30 min at 30 °C. After that, 10 mL of 0.032 mol/L Na_2S were injected into the flask dropwise. Subsequently, the mixture was stirred at 50 °C for 30 min and stirred for 1 h at 65 °C. Then the resulting 400 mL of solution were concentrated to 180 mL by a rotary evaporator at 55 °C. Finally, the resulting solution was dialyzed against water overnight. The yielded solution was referred to as CuS NPs solution.

2.3. Preparation of CuS-streptavidin

16 mL of CuS NPs solution (0.2 mg/mL) were mixed with 2.1 mL EDC/NHS aqueous solution (10 mg/mL). The mixture was incubated on a translational shaker at room temperature for 30 min to activate the –COOH groups on the surface of the nanoparticles. Then the activated CuS NPs was isolated by centrifugation for 5 min at 8000 rpm. 16 mL of HEPES (50 mmol/L, pH = 8.3) were used to dissolve the nanoparticle precipitation and then 218 μl of streptavidin (5 mg/mL) were added. After 2 h, the mixture was centrifuged to remove the unbound streptavidin. Subsequently, 16 mL of water were used to wash the CuS-streptavidin conjugate twice. Finally, the CuS-streptavidin conjugate was suspended in 1 mL of water, which was referred to as CuS-streptavidin solution.

2.4. Preparation of Ab-biotin

58.0 μl of goat anti-rabbit IgG antibody (8.76 mg/mL) were exchanged into 0.1 mol/L $NaHCO_3$ buffer by ultrafiltration and then mixed with 2 μl of biotin-XX-NHS (i.e. NHS-activated biotin with a 14 atom spacer arm) which was dissolved in DMSO at 10 mg/mL. The mixture was incubated at room temperature with gentle shaking for 3 h. The resulting mixture was dialyzed overnight against phosphate buffer

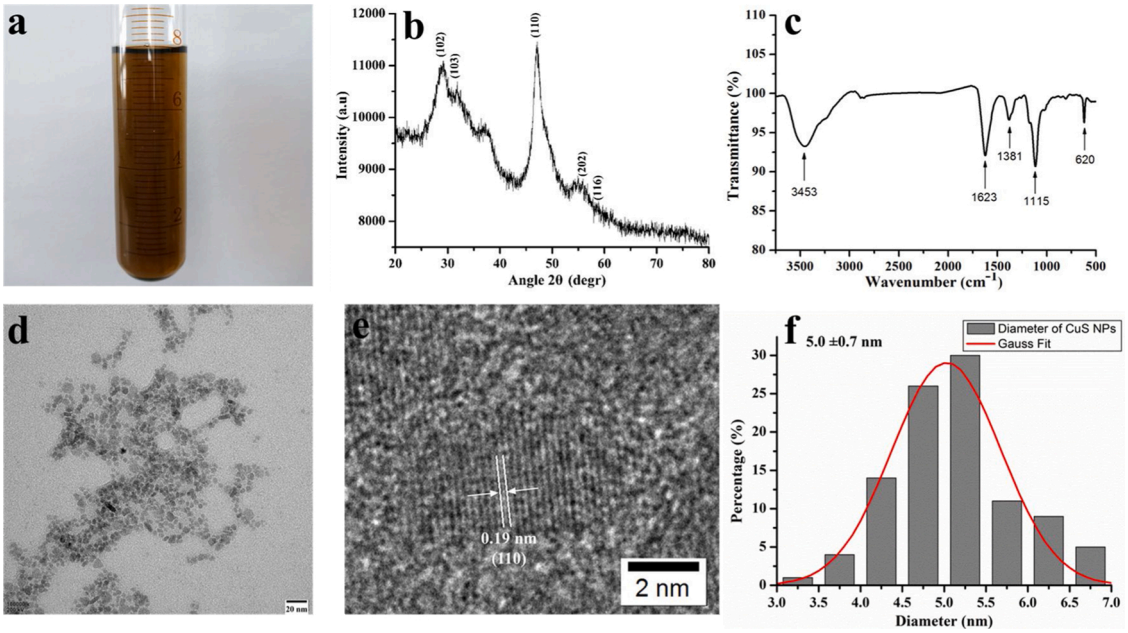

Fig. 2. Photographic image for 0.2 mg/mL of CuS nanoparticle solution (a); XRD pattern of CuS nanoparticle powder (b); FT-IR spectrum of CuS NPs (c); TEM image for CuS NPs (d); HRTEM image of CuS NPs (e); size distrubution of CuS NPs estimated from TEM image (f).

saline (PBS) and diluted to 1 mL with PBS. The resulting mixture was referred to as Ab-biotin solution and stored at 4 °C for further use.

2.5. Immunological reaction

The schematic diagram of the experimental procedure is shown in Fig. 1. 200 µl of goat anti-rabbit IgG antibody (10 µg/mL) were added into each microplate well and kept at 4 °C overnight. The wells were rinsed with water and blocked with 300 µl of PBS containing 0.1 % BSA at 37 °C for 2 h. After rinsing the wells, 200 µl of rabbit IgG standard solution or real sample were added and incubated at 37 °C for 1 h. After incubation, the wells were washed and then 200 µl of Ab-biotin (20 µg/mL) were injected to each well. After 1 h incubation at 37 °C, the wells were washed and 100 µl of CuS-streptavidin solution were added and reacted at room temperature for 30 min with shaking. After decantation of CuS-streptavidin solution, the wells were rinsed four times with water.

2.6. Preparation of analytical sample for ESR and UV–vis measurements

200 µl of DDC solution (100 *g*/L) was injected into each well, and the wells were placed in an ultrasonic bath for 30 min. Subsequently, the DDC solution in each well was transferred to a centrifuge tube. Then 300 µl of *n*-butanol were added to each well and ultrasonicated for 30 min. The *n*-butanol in the well was transferred to the same centrifuge tube, and then another 50 µl of *n*-butanol was added into the centrifuge tube. The mixture was centrifuged for 2 min at 7000 rpm to extract Cu^{2+}-DDC complex into the *n*-butanol phase. The *n*-butanol solution containing Cu^{2+}-DDC complex was referred to as the analytical sample and used in the ESR and UV–vis methods.

2.7. ESR method

An X-band Bruker A300 spectrometer was used and all the spectra were collected at room temperature. The microwave frequency was 9.85 GHz and the microwave power was 7.27 mW. The center magnetic field and the sweep width were 3450 and 500 G, respectively. The modulation amplitude was 2 G and the modulation frequency was 100 kHz. Besides, the conversion time was 80 ms, the time constant was 164 ms, and the receiver gain was 1×10^4. 40 µl of the analytical sample were injected into a glass capillary (Kimble Chase, 1.5 mm i.d., 1.8 mm o.d., 100 mm length), and the glass capillary was put into a quartz tube (Wilmad LabGlass) which was placed into the resonator cavity. While changing different samples, the quartz tube was fixed in the resonator cavity and only the glass capillary tube with the analytical sample was replaced with a long plastic tube which was attached to the top of the glass capillary. The experimental repeatability could be improved by this method. All the experiments were performed in triplicate.

2.8. UV–vis method

The UV–vis spectra were obtained on an Agilent Cary 60 UV–vis spectrophotometer at room temperature. 300 µl of the analytical sample were measured with a quartz cuvette (1 cm × 2 mm). Absorbance was recorded at 430 nm against a blank of *n*-butanol. All the experiments were performed in triplicate.

3. Results and discussion

3.1. Synthesis and characterization of CuS nanoparticles

The photograph for the synthesized CuS NPs solution is shown in Fig. 2(a). Both L-cysteine and thioglycolic acid (TGA) have been used as the ligands in the synthesis. It was found that the nanoparticles synthesized with L-cysteine were more stable and can stay in aqueous solution for more than 1 month, whereas the nanoparticles synthesized with TGA can only stay stable in aqueous solution for a few days. Thus L-cysteine was selected as the ligand.

The X-ray diffraction (XRD) analysis was performed on a Panalytical Empyrean diffractometer. The measurement was scanned with 2θ values between 20 and 80° in a speed of 3°/min. The XRD pattern of the synthesized CuS nanoparticle powder is displayed in Fig. 2(b). The XRD pattern is indexed to a hexagonal covellite CuS phase (JCPDS card No. 06-0464) [20,21]. As seen in Fig. 2(b), the diffraction peaks at 2θ values of 29.15°, 31.78°, 47.13°, 55.91°, and 61.58° can be indexed to the (102), (103), (110), (202), and (116) crystal planes of CuS, respectively. The relative broad peak width indicates that the crystallite size is small,

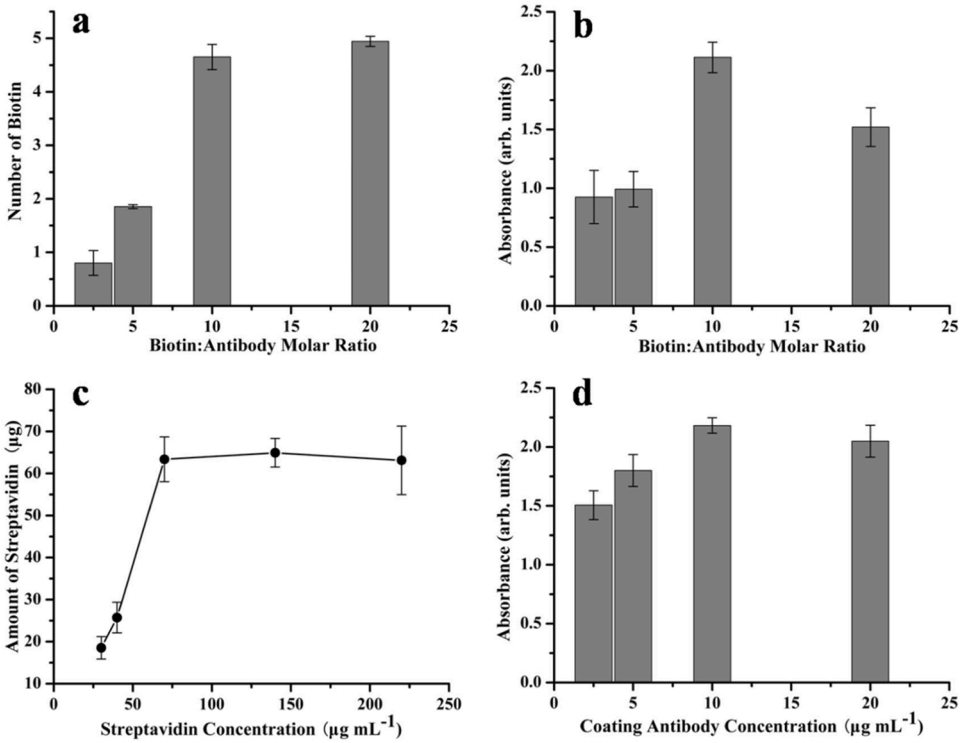

Fig. 3. Effect of molar ratio of biotin to antibody on number of biotin conjugated to each antibody (a); effect of molar ratio of biotin to antibody on absorbance obtained by UV–vis (b); effect of streptavidin concentration on amount of streptavidin attached to 1 mL of CuS NPs (c); effect of coating antibody concentration on absorbance obtained by UV–vis (d).

as is consistent with the microscope observations.

The Fourier transfer infrared (FT-IR) spectrum of CuS nanoparticle was measured by a ThermoFisher IS10 FT-IR spectroscope and is displayed in Fig. 2(c). As seen in Fig. 2(c), there is a broad absorption band peak between 3000 cm^{-1} and 3700 cm^{-1}, which corresponds to the stretching vibration of O—H and N—H of L-cysteine [20]. The absorption band at 1623 cm^{-1} is associated with the C═O stretching vibration on the carboxyl group [18,22]. The band at 620 cm^{-1} corresponds to the C–S bonding of CuS NPs [23].

The shape and morphology of the nanoparticles were observed through a JEOL JEM-2100 F field emission transmission electron microscope (TEM). The photograph collected by TEM is displayed in Fig. 2 (d) and the shape of the nanoparticles is mostly global. The CuS nanoparticles were further investigated by high-resolution transmission electron microscope (HRTEM). The HRTEM image was shown in Fig. 2 (e). The lattice spacing (0.19 nm) indicates the (110) lattice plane of hexagonal covellite CuS [24]. The size (diameter) distribution estimated from the microscope image is shown in Fig. 2(f) and the distribution is simulated with the Gauss equation. From the fitting result, the diameter of the synthesized globular CuS nanoparticles is 5.0 ± 0.7 nm.

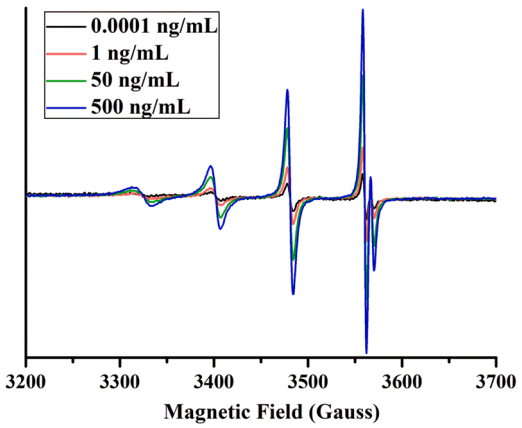

Fig. 4. ESR spectra of Cu^{2+}-DDC complex for analytical samples of different rabbit IgG concentrations.

3.2. Optimization of immunoassay experimental conditions

We have studied the effect of molar ratio of biotin to antibody on the number of biotin conjugated to each antibody. Different amount of NHS-activated biotin was mixed with the labeling antibody and the molar ratio of biotin to antibody changed from 2.5 to 20. After reacting for 3 h, the free biotin (not connected to the antibody and remained in the solution) was removed by dialysis. The biotin conjugated to the antibody was detected with HABA reagent and the number of biotin conjugated to each antibody is shown in Fig. 3(a). When the amount of NHS-activated biotin increases, the number of biotin on each antibody increases until about 4–5. As seen in Fig. 3(b), the UV–vis absorbance signal for the 100 ng/mL sample increases until the molar ratio of biotin to antibody reaches 10. When the molar ratio reaches 20, the absorbance signal decreases. High dose of biotins binding to antibody could reduce the activity of antibody when the antibody combines with antigen [25–27], as might result in the decrease of the absorbance signal. Thus the molar ratio of 10 was selected in the following experiments, and in this condition each antibody is labeled with 4.7 biotins.

To determine the maximum amount of streptavidin that can be attached to the CuS NPs, 1 mL of CuS NPs solution was first activated with EDC/NHS and then reacted with different concentrations of streptavidin for 2 h. After centrifugation, the supernatant with free streptavidin was quantified with the Coomassie brilliant blue assay. As seen in Fig. 3(c), it is found that the amount of streptavidin attached to 1 mL of CuS NPs keeps increasing and reaches a plateau when the streptavidin concentration increases to 68 μg/mL. Thus 68 μg/mL was selected as the concentration of streptavidin when reacting with CuS

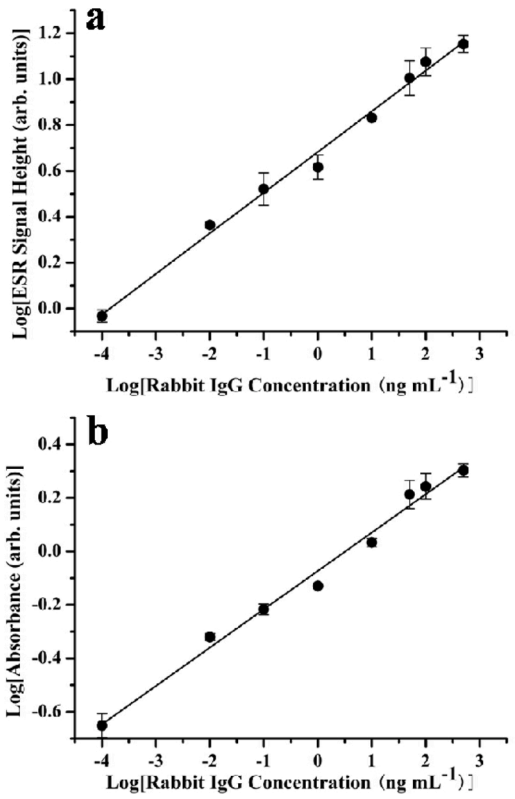

Fig. 5. Standard curves obtained by ESR (a) and UV–vis (b) methods. Error bar represents standard deviation (n = 3).

Table 1
Standard curves of the two methods.

Method	Standard equation	*r*	Liner range (ng/mL)	LOD (pg/mL)
ESR	y = 0.177x + 0.683	0.996	0.0088–500	1.76
UV–vis	y = 0.143x - 0.073	0.993	0.0118–500	2.36

nanoparticles.

The effect of the coating antibody concentration on the UV–vis absorbance signal was studied when the antigen concentration was 100 ng/mL. As seen in Fig. 3(d), the signal slightly increases when the coating antibody concentration increases from 2.5 to 10 μg/mL and when the antibody concentration is higher than 10 μg/mL, the signal stays unchanged. Thus 10 μg/mL was used as the optimal concentration of coating antibody.

3.3. Standard curves

The cupric ions were easily released from the nanoparticles with the help of DDC and *n*-butanol. Any Cu^{+} possibly existing inside the nanoparticles would be oxidized to Cu^{2+} when DDC was added and Cu^{2+}-DDC complex formed. The ESR spectra of Cu^{2+}-DDC complex for the 0.0001, 1, 50, and 500 ng/mL analyts are displayed in Fig. 4. The signal height (i.e. peak-to-peak amplitude) of the third peak is used to represent the magnitude of the ESR signal. As seen in Fig. 4, there is a split in the fourth peak in the ESR spectrum possibly caused by the different magnetic moments of the two isotopes of cupric ion (i.e. Cu^{63} and Cu^{65}) [28,29]. As the antigen rabbit IgG concentration increases, the ESR signal of Cu^{2+}-DDC complex also increases. The logarithm of the ESR signal versus the logarithm of rabbit IgG concentration is plotted in Fig. 5(a). The standard curve is simulated with a linear equation and the fitting parameters are listed in Table 1. The standard curve is well fitted linearly and the correlation coefficient (*r*) is 0.996. The LOD is 1.76 pg/mL, which is calculated by 2SD/initial slope and SD is the standard deviation estimated with the 0.01 ng/mL analyte (n = 7).

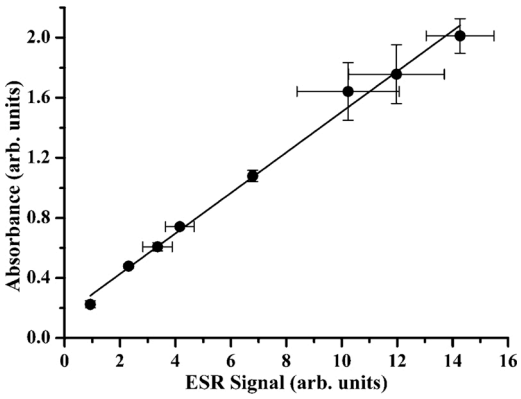

Fig. 6. Correlation of measurement signals at the same analyte concentrations obtained by ESR and UV–vis methods. Error bar represents standard deviation (n = 3).

Table 2
Comparison of analytical performance with other published works.

Method	Analyte	Sensitivity	Detection range	Reference
ESR biosensor	Rabbit IgG	1.76 pg/mL	0.0088–500 ng/mL	Present work
Electrochemcial biosensor	Human IgG	1.2 fg/mL	0.0005–500000 pg/mL	[32]
Surface-enhanced Raman scattering (SERS)	Human IgG	0.05 pg/mL	0.0001–10 ng/mL	[33]
Enzyme-linked immunosorbent assay (ELISA)	Human IgG	0.86 pg/mL	0.001–100 ng/mL	[9]
Lateral flow immunoassays (LFIs)	Rabbit IgG	5 pg/mL	0.05–10 ng/mL	[35]
Electrochemcial biosensor	Human IgG	30 pg/mL	0.1–10 ng/mL	[36]
Fluorescence biosensor	Pig IgG	31 pg/mL	0.75–23.50 ng/mL	[10]
Fluorescence biosensor	Human IgG	34.5 pg/mL	0.13–1.50 ng/mL	[37]
Enzyme-linked immunosorbent assay (ELISA)	Human IgG	50 pg/mL	0.1–10 ng/mL	[38]
Surface-enhanced Raman scattering (SERS)	Human IgG	90 pg/mL	0.09–90 ng/mL	[39]
Optoelectrical biosensor	Human IgG	14 ng/mL	25-25,000 ng/mL	[40]
Surface plasmon resonance (SPR)	Human IgG	40 ng/mL	5–30 μg/mL	[41]
Optical fiber biosensor	Anti-goat IgG	200 ng/mL	4–200 μg/mL	[42]
Optical fiber sensor	Anti-mouse IgG	600 ng/mL	1–40 μg/mL	[43]

For the standard curve obtained from the UV–vis spectrometry, the logarithm of the absorbance versus the logarithm of rabbit IgG concentration is plotted in Fig. 5(b). As listed in Table 1, the standard curve is well fitted using a linear equation with a high correlation coefficient ($r = 0.993$). The LOD is 2.36 pg/mL. The correlationship between the signal at the same analyte concentration obtained by the ESR and UV–vis methods is plotted in Fig. 6 and the high *r* value (0.996) indicates that the measurement results obtained by the two methods are well correlated.

3.4. Analytical performance

The detection range of the ESR method is from 8.8 pg/mL to 500 ng/mL. With this new method, rabbit IgG could be detected within a wide range of concentrations which spread over almost 5 magnitude orders.

The reproducibility of the present method was evaluated by measuring the relative standard deviations (RSDs) of the intra-assay and inter-assay experiments. The intra-assay tests were performed by measuring five parallel analytical samples, whereas the inter-assay tests were performed by measuring five samples prepared from different batch work. The RSDs from the intra- and inter-assay tests are respectively 3.4 and 11.2 % for the ESR method and 2.8 and 13.5 % for the UV–vis method. Thus the reproducibility of the present method is satisfactory.

We have developed two ESR immunoassay methods previously and applied the methods in the detection of rabbit IgG. In the first method [30], 10 and 30 nm iron oxide nanoparticles were used as the probe to label the antibody and the signal from the iron oxide nanoparticles was recorded by the ESR spectrometer. The LOD of the method for detecting rabbit IgG was 14 ng/mL. In the second method [31], 180 nm iron oxide nanoparticles were used as the probe to label the antibody and the LOD for detecting rabbit IgG was 130 ng/mL. Compared with our previously developed methods, the LOD of the present method has been improved for 4–5 orders of magnitude.

The analytical performance (sensitivity and detection range) of this work was also compared with some other publications on IgG detection, and the comparison is listed in Table 2. As seen in Table 2, the sensitivity of the reported studies ranges from 1.2 fg/mL to 600 ng/mL, and the detection range reported in the publications ranges from 1 to 9 orders of magnitude. The sensitivity of the electrochemical immunoassay method described by Qin et al. is 1.2 fg/mL, and the detection range spreads over 9 orders of magnitude [32]. The sensitivity and detection range of the method developed by Qin et al. are far better than the other methods listed in Table 2. Besides, the sensitivity of the method reported by Karn-orachai et al. is 0.05 pg/mL, which is higher than our method [33]. The sensitivity of the present method (1.76 pg/mL) is satisfactory. In the present method, the detection range spreads over almost 5 orders of magnitudes. Compared with other methods, such detection range is wide enough. Therefore, the analytical performance of this ESR immunoassay method is satisfactory when comparing with the existing immunoassay methods.

Besides, CuS NPs were synthesized with $Cu(NO_3)_2$, $Na_2S{\cdot}9H_2O$, and L-cysteine, which are easily available and at low cost. The synthesis of CuS NPs with mild synthesis conditions is relatively simple, time-saving, and eco-friendly. Cu^{2+} is isolated from the sample matrix and extracted into the organic phase, which can effectively avoid the endogenous interferences from the real sample. There is no ESR signal in most biological materials so that the background signal does not exist. Compared with traditional enzyme-linked immunosorbent assay (ELISA) method, ESR spectroscopy which detects paramagnetic metal ions (e.g. Cu^{2+}) would not be interfered by the color of the analytical sample. The analytical samples are also very stable and insensitive to heat and light so that the results of the analytical samples within at least 2 weeks are repeatable. Compared with the UV–vis method, the ESR method can measure the analytical samples with no dilution. As for UV–vis method, the analytical sample should be diluted when its concentration is too high (absorbance>1). ESR spectroscopy is a technique that is unique to detect unpaired electrons. When the ESR method was applied, the resonance signal from Cu^{2+} was measured, and any impurities from sample itself will not affect the quantification. However, the UV–vis absorbance might be influenced when the real sample is complicated. In addition, the sample volume required for the ESR method is only 40 μl, which is over 5 times less than that of the UV–vis method.

Table 3
Analytical results of the spiked serum samples by ESR method.

Spiked (ng/mL)	Found (ng/mL)	Recovery (%)	RSD (n = 3, %)
10.00	11.37 ± 1.92	113.7	16.9
40.00	43.28 ± 1.33	108.2	3.1

3.5. Analysis of real rabbit serum samples

The present method was applied to the determination of the rabbit IgG in the real rabbit serum. The rabbit serum was directly diluted with PBS buffer and analyzed according to the above mentioned experimental procedures. The rabbit IgG concentration in the rabbit serum was found to be 7.76 and 7.50 mg/mL respectively by the ESR and UV–vis methods. The results are consistent with the reported 5−10 mg/mL in the previous publications [34].

Recovery experiments were performed in order to examine the accuracy of the present method. The spiked samples were prepared by adding 10 and 40 ng/mL rabbit IgG standard solution into the diluted rabbit serum. The results are listed in Table 3. The recoveries were respectively 113.7 and 108.2 % when the spiked concentrations were 10 and 40 ng/mL. The results indicate that the recovery percentage is in the acceptable range and the present method can be applied to the analysis of real serum samples.

4. Conclusions

In this work, we have presented a novel ESR method for immunoassay using synthesized CuS nanoparticles as the probe, and rabbit IgG was used as the model antigen to examine the performance of this new method. The method is highly sensitive when detecting rabbit IgG with a limit of detection as low as 1.76 pg/mL. Also the method has a wide range of detecting concentration spreading over almost 5 orders of magnitude, and in this wide range the logarithm of the signal increases linearly with the logarithm of the antigen concentration. The method has good reproducibility proved by the intra- and inter-assay experiments as well as good accuracy when being applied to the analysis of real rabbit serum sample.

CRediT authorship contribution statement

Sizhu Tian: Methodology, Formal analysis, Investigation, Writing - original draft. **Xuwen Li:** Supervision. **Jia Jiang:** Investigation. **Li Tang:** Investigation. **Hanqi Zhang:** Methodology, Writing - review & editing. **Yong Yu:** Funding acquisition, Project administration. **Ziwei Zhang:** Conceptualization, Funding acquisition, Writing - review & editing.

Declaration of Competing Interest

The authors declare that they have no known competing financial interests or personal relationships that could have appeared to influence the work reported in this paper.

Acknowledgements

This work was supported by the Science and Technology Development Planning Project of Jilin Province (Grant Nos. 20180201027GX and 20180201059SF).

References

[1] L.K. Aminov, M.R. Gafurov, S.L. Korableva, I.N. Kurkin, A.A. Rodionov, Superhyperfine structure of the ESR spectra of Gd3+ impurity ions in LiYF4 double fluoride, Phys. Solid State 59 (2017) 564–568.
[2] J. Jiang, S. Zang, D. Li, K. Wang, S. Tian, A. Yu, Z. Zhang, Determination of antioxidant capacity of thiol-containing compounds by electron spin resonance spectroscopy based on Cu(2+) ion reduction, Talanta 184 (2018) 23–28.

[3] P.P. Borbat, A.J. Costa-Filho, K.A. Earle, J.K. Moscicki, J.H. Freed, Electron spin resonance in studies of membranes and proteins, Science 291 (2001) 266.
[4] D.V. Ananchenko, S.V. Nikiforov, S.F. Konev, G.R. Ramazanova, ESR and luminescent properties of anion-deficient α-Al2O3 single crystals after high-dose irradiation by a pulsed electron beam, Opt. Mater. 90 (2019) 118–122.
[5] S. Zang, S. Tian, J. Jiang, D. Han, X. Yu, K. Wang, D. Li, D. Lu, A. Yu, Z. Zhang, Determination of antioxidant capacity of diverse fruits by electron spin resonance (ESR) and UV-vis spectrometries, Food Chem. 221 (2017) 1221–1225.
[6] I.A. Darwish, Immunoassay methods and their applications in pharmaceutical analysis: basic methodology and recent advances, Int. J. Biomed. Sci. 2 (2006) 217–235.
[7] N. Chiem, D.J. Harrison, Microchip-based capillary electrophoresis for immunoassays: analysis of monoclonal antibodies and theophylline, Anal. Chem. 69 (1997) 373–378.
[8] R. Liu, S. Zhang, C. Wei, Z. Xing, S. Zhang, X. Zhang, Metal stable isotope tagging: renaissance of radioimmunoassay for multiplex and absolute quantification of biomolecules, Acc. Chem. Res. 49 (2016) 775–783.
[9] K. Zeng, S. Tian, Z. Wang, C. Shen, J. Luo, M. Yang, Y.-N. Liu, An ELISA for the determination of human IgG based on the formation of a colored iron(II) complex and photometric or visual read-out, Microchim. Acta. 184 (2017) 2791–2796.
[10] Q. Zhao, Q. Wu, P. Ma, L. Xu, F. Zhang, D. Li, X. Liu, S. Xu, Y. Sun, D. Song, X. Wang, Selective and sensitive fluorescence detection method for pig IgG based on competitive immunosensing strategy and magnetic bioseparation, Talanta 195 (2019) 103–108.
[11] R.K. Leute, E.F. Ullman, A. Goldstein, L.A. Herzenberg, Spin immunoassay technique for determination of morphine, Nat. New Biol. 236 (1972) 93–94.
[12] G.K. Humphries, H.M. McConnell, Immune lysis of liposomes and erythrocyte ghosts loaded with spin label, Proc. Natl. Acad. Sci. U. S. A. 71 (1974) 1691–1694.
[13] J.C. Hsia, C.T. Tan, Membrane immunoassay: principle and applications of spin membrane immunoassay, Ann. N. Y. Acad. Sci. 308 (1978) 139–148.
[14] T. Matsuo, H. Shinzawa, H. Togashi, M. Aoki, K. Sugahara, K. Saito, T. Saito, T. Takahashi, I. Yamaguchi, M. Aoyama, H. Kamada, Highly sensitive hepatitis B surface antigen detection by measuring stable nitroxide radical formation with ESR spectroscopy, Free Radic. Biol. Med. 25 (1998) 929–935.
[15] G. Ku, M. Zhou, S. Song, Q. Huang, J. Hazle, C. Li, Copper sulfide nanoparticles as a new class of photoacoustic contrast agent for deep tissue imaging at 1064 nm, ACS Nano 6 (2012) 7489–7496.
[16] G.C. Fan, H. Zhu, D. Du, J.R. Zhang, J.J. Zhu, Y. Lin, Enhanced photoelectrochemical immunosensing platform based on CdSeTe@CdS:Mn core-shell quantum dots-sensitized TiO2 amplified by CuS nanocrystals conjugated signal antibodies, Anal. Chem. 88 (2016) 3392–3399.
[17] A.K. Dutta, S. Das, S. Samanta, P.K. Samanta, B. Adhikary, P. Biswas, CuS nanoparticles as a mimic peroxidase for colorimetric estimation of human blood glucose level, Talanta 107 (2013) 361–367.
[18] L. Liang, S. Peng, Z. Yuan, C. Wei, Y. He, J. Zheng, Y. Gu, H. Chen, Biocompatible tumor-targeting nanocomposites based on CuS for tumor imaging and photothermal therapy, RSC Adv. 8 (2018) 6013–6026.
[19] Y. Guo, X. Guan, L. Li, X. Chen, P. Wang, Syntheses of water-soluble CuS nanocrystals and interaction between biological macromolecule function, J. Nanyang Normal Univ. 8 (2019) 44–46.
[20] S.M.M. Nelwamondo, M.J. Moloto, R.W.M. Krause, N. Moloto, Synthesis and characterization of alanine-capped water soluble copper sulphide quantum dots, Mater. Lett. 75 (2012) 161–164.
[21] S.M.M. Nelwamondo, M.J. Moloto, R.W. Krause, N. Moloto, Direct synthesis of water soluble CuS and CdS nanocrystals with hydrophilic glucuronic and thioglycolic acids, Mater. Res. Bull. 47 (2012) 4392–4397.
[22] Y.D. Zhu, J. Peng, L.P. Jiang, J.J. Zhu, Fluorescent immunosensor based on CuS nanoparticles for sensitive detection of cancer biomarker, Analyst 139 (2014) 649–655.
[23] D.B. Malavekar, V.C. Lokhande, V.J. Mane, S.B. Ubale, U.M. Patil, C.D. Lokhande, Enhanced energy density of flexible asymmetric solid state supercapacitor device fabricated with amorphous thin film electrode materials, J. Phys. Chem. Solids 141 (2020), 109425.
[24] Z. Hosseinpour, A. Alemi, A.A. Khandar, X. Zhao, Y. Xie, A controlled solvothermal synthesis of CuS hierarchical structures and their natural-light-induced photocatalytic properties, New J. Chem. 39 (2015) 5470–5476.
[25] N. Liu, D. Nie, Z. Zhao, X. Meng, A. Wu, Ultrasensitive immunoassays based on biotin–streptavidin amplified system for quantitative determination of family zearalenones, Food Control 57 (2015) 202–209.
[26] Z. Lin, X. Wang, Z.J. Li, S.Q. Ren, G.N. Chen, X.T. Ying, J.M. Lin, Development of a sensitive, rapid, biotin-streptavidin based chemiluminescent enzyme immunoassay for human thyroid stimulating hormone, Talanta 75 (2008) 965–972.
[27] Y. Li, Y. Wang, P. Li, Y. Zhang, Y. Ke, W. Yu, K. Wen, S. Ding, Z. Wang, X. Yu, High efficient chemiluminescent immunoassays for the detection of diclazuril in chicken muscle based on biotin–streptavidin system, Food Agric. Immunol. 31 (2020) 255–267.
[28] D. Li, J. Jiang, D. Han, X. Yu, K. Wang, S. Zang, D. Lu, A. Yu, Z. Zhang, Measurement of antioxidant capacity by Electron spin resonance spectroscopy based on copper(II) reduction, Anal. Chem. 88 (2016) 3885–3890.
[29] S. Tian, X. Li, J. Jiang, K. Wang, H. Zhang, A. Yu, Z. Zhang, Application of Cu(2+)-based electron spin resonance spectroscopy in measurement of antioxidant capacity of fruits, Anal. Bioanal. Chem. 411 (2019) 6677–6686.
[30] J. Jiang, S. Tian, K. Wang, Y. Wang, S. Zang, A. Yu, Z. Zhang, Electron spin resonance spectroscopy for immunoassay using iron oxide nanoparticles as probe, Anal. Bioanal. Chem. 410 (2018) 1817–1824.
[31] S. Tian, J. Jiang, S. Zang, K. Wang, Y. Yu, X. Li, H. Zhang, A. Yu, Z. Zhang, Determination of IgG by electron spin resonance spectroscopy using Fe3O4 nanoparticles as probe, Microchem. J. 141 (2018) 444–450.
[32] X. Qin, Y. Sui, A. Xu, L. Liu, Y. Li, Y. Tan, C. Chen, Q. Xie, Ultrasensitive immunoassay of proteins based on in-situ enzymatic formation of quantum dots and microliter-droplet anodic stripping voltammetry, J. Electroanal. Chem. 811 (2018) 121–127.
[33] K. Karn-orachai, K. Sakamoto, R. Laocharoensuk, S. Bamrungsap, T. Dharakul, K. Miki, SERS-based immunoassay on 2D-arrays of Au@Ag core–shell nanoparticles: influence of the sizes of the SERS probe and sandwich immunocomplex on the sensitivity, RSC Adv. 7 (2017) 14099–14106.
[34] H.M. Farrell Jr, R. Jimenez-Flores, G.T. Bleck, E.M. Brown, J.E. Butler, L. K. Creamer, C.L. Hicks, C.M. Hollar, K.F. Ng-Kwai-Hang, H.E. Swaisgood, Nomenclature of the proteins of cows' milk–sixth revision, J. Dairy Sci. 87 (2004) 1641–1674.
[35] J. Zhang, Q. Yu, W. Qiu, K. Li, L. Qian, X. Zhang, G. Liu, Gold-platinum nanoflowers as a label and as an enzyme mimic for use in highly sensitive lateral flow immunoassays: application to detection of rabbit IgG, Mikrochim. Acta 186 (2019) 357.
[36] S. Dong, M. Tong, D. Zhang, T. Huang, The strategy of nitrite and immunoassay human IgG biosensors based on ZnO@ZIF-8 and ionic liquid composite film, Sens. Actuators B Chem. 251 (2017) 650–657.
[37] Q. He, X. Chen, Y. He, T. Guan, G. Feng, B. Lu, B. Wang, X. Zhou, L. Hu, D. Cao, Spectral-optical-tweezer-assisted fluorescence multiplexing system for QDs-encoded bead-array bioassay, Biosens. Bioelectron. 129 (2019) 107–117.
[38] L. Wu, M. Zhang, L. Zhu, J. Li, Z. Li, W. Xie, Nanozyme-linked immunosorbent assay for porcine circovirus type 2 antibody using HAuCl4/H2O2 coloring system, Microchem. J. 157 (2020), 105079.
[39] A. Ali, E.Y. Hwang, J. Choo, D.W. Lim, Nanoscale graphene oxide-induced metallic nanoparticle clustering for surface-enhanced Raman scattering-based IgG detection, Sens. Actuators B Chem. 255 (2018) 183–192.
[40] S. Mas, A.A. Badran, M.J. Juarez, D.H. Fernandez de Rojas, S. Morais, A. Maquieira, Highly sensitive optoelectrical biosensor for multiplex allergy diagnosis, Biosens. Bioelectron. 166 (2020), 112438.
[41] Q. Wang, B.-T. Wang, Surface plasmon resonance biosensor based on graphene oxide/silver coated polymer cladding silica fiber, Sens. Actuators B Chem. 275 (2018) 332–338.
[42] Y. Cardona-Maya, A.B. Socorro, I. Del Villar, J.L. Cruz, J.M. Corres, J.F. Botero-Cadavid, Label-free wavelength and phase detection based SMS fiber immunosensors optimized with cladding etching, Sens. Actuators B Chem. 265 (2018) 10–19.
[43] A. Vicente, D. Santano, P. Zubiate, A. Urrutia, I. Del Villar, C.R. Zamarreño, Lossy mode resonance sensors based on nanocoated multimode-coreless-multimode fibre, Sens. Actuators B Chem. 304 (2020), 126955.

Sizhu Tian is pursuing her PhD degree in College of Chemistry, Jilin University. Her research interest focuses on immunoassay and synthesis metal nanoparticles with electron spin resonance signal.

Xuwen Li is currently a professor in Jilin University. His research interest focuses on spectral and chromatography analysis.

Jia Jiang received his PhD degree in College of Chemistry, Jilin University in 2018. His research interest is biosensing and immunoassay.

Li Tang is pursuing her Master degree in College of Chemistry, Jilin University. Her research area is analytical chemistry.

Hanqi Zhang is a professor in Jilin University. His research interest focuses on spectral analysis, chromatography analysis, and instrumentation.

Yong Yu received his PhD degree in College of Chemistry, Jilin University. He is currently an associate professor in Jilin University. His research interest focuses on chromatography analysis and instrumentation.

Ziwei Zhang received his PhD degree in biophysics in Cornell University in 2010. She is currently an associate professor in Jilin University. Her research interest focuses on spectral analysis, chromatography analysis, and electron spin resonance spectroscopy.